Chemical Science

RSC Publishing

EDGE ARTICLE

View Article Online
View Journal | View Issue

Cite this: *Chem. Sci.*, 2013, **4**, 1270

Pinning down the solid-state polymorphism of the ionic liquid [bmim][PF_6]†

Sofiane Saouane,[a] Sarah E. Norman,[b] Christopher Hardacre*[b] and Francesca P. A. Fabbiani*[a]

Received 11th November 2012
Accepted 21st December 2012

DOI: 10.1039/c2sc21959j

www.rsc.org/chemicalscience

The solid-state polymorphism of the ionic liquid 1-butyl-3-methylimidazolium hexafluorophosphate, [bmim][PF_6], has been investigated *via* low-temperature and high-pressure crystallisation experiments. The samples have been characterised by single-crystal X-ray diffraction, optical microscopy and Raman spectroscopy. The solid-state phase behaviour of the compound is confirmed and clarified with respect to previous phase diagrams. The structures of the previously reported γ-form, which essentially exhibits a G′T cation conformation, as well as those of the elusive β- and α-forms, are reported. Crystals of the β-phase are twinned and the structure is heavily disordered; the cation conformation in this form is predominantly TT, though significant contributions from other less frequently encountered conformers are also observed at low temperature and high pressure. The cation conformation in the α-form is GT; the presence of the G′T conformer at 193 K in this phase can be eliminated on cooling to 100 K. Whilst X-ray structural data are overall in good agreement with previous interpretations based on Raman and NMR studies, they also reveal a more subtle interplay of intermolecular interactions, which give rise to a wider range of conformers than previously considered.

Introduction

Due to their unique physicochemical properties, room-temperature ionic liquids (ILs) have attracted considerable interest in several branches of chemistry and chemical engineering. A low melting point, large liquid range and high thermal stability are some of the properties that make them attractive green solvents for synthetic and catalytic processes.[1–3] More recently, ILs have found application as crystallisation media. Although their nonvolatility makes them poor solvents for crystallisation by evaporation, they can be used in solvothermal, thermal shift, co-solvent, slow diffusion and electrocrystallisation of a variety of chemicals, including pharmaceuticals and biomolecules.[4–6]

The liquid structure of ILs has been the subject of numerous theoretical and experimental investigations, the latter focusing on X-ray and neutron scattering experiments.[7–9] The X-ray crystal structures of the most common ILs have also been reported in the literature: the Cambridge Structural Database[10] (the CSD, V. 5.33 including updates to May 2012 was searched for structure with 3-D coordinates, an *R*-factor below 10% and no errors) contains 212 structures of 1-methylimidazolium-based salts, of which 90 have a confirmed melting point below 373 K, which is the commonly accepted maximum melting temperature for defining an IL. Crystal polymorphism in 1,3-dialkylimidazolium-based ILs has been reported on the basis of spectroscopic, diffraction and calorimetric data. To the best of our knowledge, the first example also confirmed by single-crystal X-ray diffraction was that of [bmim]Cl.[11]

1-Butyl-3-methylimidazolium hexafluorophosphate, [bmim][PF_6], (Fig. 1), is one of the most studied ionic liquids. A wide range of simulations have been undertaken on this compound and show significant probability of finding anions around the C2 hydrogen position as well as above and below the plane of the imidazolium ring.[12,13] As found with other ionic liquids, such as the analogous chloride based systems,[14,15] steric hindrance from the long alkyl chain, in this case butyl, has an

[a]*GZG, Abteilung Kristallographie, Georg-August-Universität Göttingen, Göttingen, 37077, Germany. E-mail: ffabbia@gwdg.de; Fax: +49 551 399521; Tel: +49 551 393935*

[b]*School of Chemistry and Chemical Engineering, The QUILL Centre, Queen's University Belfast, Belfast BT9 5AG, UK. E-mail: c.hardacre@qub.ac.uk; Fax: +44 (0)28 90 974687; Tel: +44 (0)28 90 974592*

† Electronic supplementary information (ESI) available: Crystallographic data processing and structure refinement details, anion disorder, geometric parameters describing cation dimers, cation and anion coordination numbers and environment, short H···F contacts and simulated powder patterns for the three polymorphs. CCDC reference numbers 909171–909175. For ESI and crystallographic data in CIF or other electronic format see DOI: 10.1039/c2sc21959j

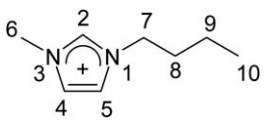

Fig. 1 Chemical diagram of the $[bmim]^+$ cation with atom numbering scheme.

effect on the structure with the probability of anion interaction with the other ring hydrogens being dominated by the one closest to the methyl group. The solid-state behaviour of [bmim][PF_6] at ambient-pressure conditions has been extensively studied by a variety of techniques, including Raman and NMR spectroscopy, calorimetry, single-crystal X-ray diffraction, as well as wide-angle X-ray scattering. [bmim][PFB_6] has also been the subject of high-pressure Raman and calorimetry experiments. Despite the evidence for crystal polymorphism, only one crystal structure has been reported in the literature to date.[16,17] A brief summary of the findings to date is given in Table 1, emphasising the conditions under which different phases have been obtained and using the scheme introduced by Endo *et al.*[18] as reference to harmonising the polymorph nomenclature.

Endo *et al.*[18,19] characterised three crystalline forms, α, β and γ, by calorimetry, Raman and NMR spectroscopy, pointing out that the endothermic transition to the γ-phase is difficult to detect by DSC measurements. The authors assigned the cation structure in the three phases by comparing experimental Raman spectra with calculated ones obtained by full geometry optimisation, using DFT methods, of the three most stable rotational isomers of the $[bmim]^+$ cation, GT, TT and G′T (see Results and discussion section for details). The isomers were identified on the basis of the conformations found in experimental crystal structures and in gas-phase quantum chemical calculations.[20] According to their Raman spectra, Endo *et al.* assigned the conformers of the α-, β- and γ-phases as GT, TT and G′T, respectively.

The most recent and comprehensive high-pressure investigation into the polymorphism of [bmim][PF_6] was carried out by means of Raman spectroscopy up to *ca.* 1 GPa by Russina *et al.*[21] Raman work was also carried out by Yoshimura *et al.*[22] and by Su *et al.* up to 2 GPa;[23] Su *et al.* have also carried out differential thermal analysis experiments up to 1 GPa.[24] Russina *et al.*

Table 1 Summary of crystallisation conditions and observed polymorphs of [bmim][PF_6] reported in the literature to date

Author	Experiments[a]	Crystallisation conditions and observed crystalline phases[b]		
Endo *et al.*[18]	LT Raman, DSC	**α-form** Cool to 192 K, heat and crystallise at 226.5 K	**β-form** Phase transition on heating α to 250.3 K	**γ-form** Phase transition on heating β to 276 K
Triolo *et al.*[9]	LT DSC, WAXS	**cr-II** Heat supercooled liquid and crystallise at 220 K	n.o.[c]	**cr-I** Phase transition on heating cr-II to 245–252 K, or cooling to 260 K and waiting a few hours. WAXS pattern matches structures of Dibrov *et al.* and Choudhry *et al.*
		Note: In the first part of the paper the phase assignment on the basis of comparison with single-crystal structures is reversed to the one given later		
Choudhry *et al.*[17]	LT DSC, SC-XRD	Cool to 123 K, crystallise at 233 K (evidence from DSC curve)	Evidence of α → β transition at 263 K from DSC[d]	Cool to 123 K, crystallise at 233 K and grow at 243 K. β → γ transition at 276 K from DSC[d]
Dibrov and Kochi.[16]	LT SC-XRD	n.o.	n.o.	Shock-induced crystallisation after supercooling to 243 K
Russina *et al.*[21]	HP Raman to 0.9 GPa	**S1** Keep at 0.44 GPa for 12 hours; crystallise on further pressurisation	**S2** Depressurise S1 to 0.04 GPa	n.o.
Su *et al.*[23,24]	HP Raman to 2 GPa, DTA to 1 GPa	Only one phase reported in both papers; re-analysis of the Raman spectra by Russina *et al.* points out evidence for S1 → S2		n.o.
Yoshimura *et al.*[22]	HP Raman to 2 GPa	Identified as S1 by Russina *et al.*	n.o.	n.o.
This work	HP Raman and XRD to 0.8 GPa; LT Raman and SC-XRD; optical microscopy	**α-form** Flash-cool below glass transition, heat and crystallise at 228 K. Compression of β-form above 0.4 GPa	**β-form** Phase transition on heating α to 248 K. Crystallise at high pressure below 0.4 GPa	**γ-form** Phase transition on heating α or β between 248 and 258 K; isothermal crystallisation of the liquid at 277 K. Crystallise from an aq. mix at 0.8 GPa

[a] LT = low temperature; HP = high pressure; DSC = differential scanning calorimetry; WAXS = wide-angle X-ray scattering; SC-XRD: single-crystal X-ray diffraction; DTA = differential thermal analysis. [b] Bold-face phases identified in original publications. [c] n.o. = not observed/reported. [d] Current interpretation of DSC signal.

identified two high-pressure phases by Raman spectroscopy and constructed an elegant phase diagram; at ambient temperature, they determined a crystallisation pressure of *ca.* 0.048 GPa for the phase corresponding to the β-polymorph of Endo *et al.*, in excellent agreement with a value of *ca.* 0.04 GPa reported by acoustic measurements.[25] A second high-pressure phase, which the authors obtained by ambient-temperature crystallisation above *ca.* 0.44 GPa, was assigned the GT conformer and identified as the α-phase of Endo *et al.* The preference of this conformer at high pressure was confirmed in a very recent molecular dynamics simulation study, albeit in the liquid state.[26]

Intrigued by the observations that polymorphism of [bmim][PF_6] was reported at both low-temperature and high-pressure conditions yet only one crystal structure is available in the CSD, our approach has been to explore how the high-pressure and low-temperature crystallisation of [bmim][PF_6] might lead to the formation of new polymorphs and to elucidate the crystal structures of these polymorphs by single-crystal X-ray diffraction, complementing the results with Raman spectroscopy.

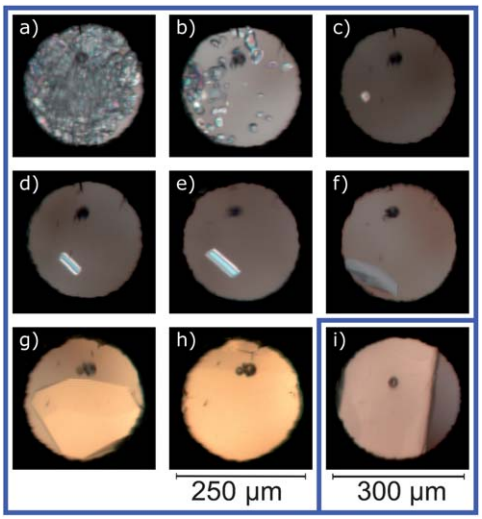

Fig. 2 Stages of isothermal *in situ* crystal growth of the β-phase of [bmim][PF_6] in the DAC at 293 K. (a) and (b): melting at *ca.* 0.09 GPa; (c)–(g): slow growth on increasing pressure; (h): final crystal at 0.35 GPa (crystal 1); (i): final crystal at 0.07 GPa (crystal 2) in equilibrium with the liquid phase.

Experimental methods

Material

The title compound was prepared in house. Bromobutane (1.1 eq.) was added to a stirred solution of methyl imidazole (1 eq.) in acetonitrile. The resulting mixture was stirred at 343 K overnight. After cooling, the solvent was concentrated and the crude product was recrystallised from ethyl acetate to yield a pale yellow solid. The bromide salt was then redissolved in acetonitrile and potassium hexfluorophosphate (1.1 eq.) was added and the suspension was stirred vigorously overnight. The mixture was then filtered and the solvent concentrated *in vacuo*. The resulting oil was then redissolved in DCM and refiltered to remove the KBr byproduct. Finally, the DCM solution was flushed through a pad of silica/alumina and charcoal and concentrated *in vacuo* to yield a colourless liquid. The ^{1}H, ^{31}P and ^{13}C-NMR were consistent with previous reports. The ionic liquid was dried for 4 h at 333 K under high vacuum before use.

High-pressure crystallisation: α- and β-phases

A square-shaped beryllium-free diamond-anvil cell (DAC) of the Ahsbahs type[27] (45° half-cell opening angle) was used for the high-pressure experiments; the cell was equipped with 600 μm culet diamonds of low fluorescence grade and Inconel gaskets with a starting diameter hole of 300 μm. The pressure inside the sample chamber was measured according to the ruby fluorescence method[28] using an in-house built kit that has a precision of 0.05 GPa. Crystallisation was induced by increasing the pressure progressively to *ca.* 0.7 GPa. A single crystal was obtained by slow melting of the resulting polycrystalline powder when releasing the pressure to *ca.* 0.09 GPa (isothermal crystal growth) and subsequently increasing the pressure until the crystal was as big as the gasket hole (Fig. 2). The final pressure inside the sample chamber was 0.35 GPa. A second single crystal was obtained by cooling the loaded DAC at 0.4 GPa for 12 h at 277 K and subsequently warming it to room temperature and adjusting the pressure for optimal crystal growth. The final crystal at *ca.* 0.07 GPa was in equilibrium with the liquid and X-ray diffraction data were collected at phase boundary conditions (Fig. 2). Both single crystals were attributed to the β-form. Despite the larger standard uncertainty, our value for the crystallisation pressure is in good agreement with that of 0.048(25) GPa by Russina *et al.*[21] On compressing the single crystals to pressures above *ca.* 0.4 GPa, a phase transition accompanied by the disintegration into polycrystalline material was observed. Analysis of this phase at 0.8 GPa by Raman spectroscopy revealed the presence of the α-phase.

Crystallisation in capillaries: α- and β-phases

Initial crystallisation experiments were performed by loading the sample in 0.3 mm glass capillaries. The capillaries were sealed to keep the sample dry. The sample was rapidly flash cooled by immersing the capillary in liquid nitrogen to induce the crystallisation of a glass. On warming, a liquid-mediated transition to needle-like crystals was observed; on further warming these needles transformed to plate-like crystals. A single crystal was then grown by temperature cycling; the capillary was subsequently transferred to a Bruker Apex diffractometer equipped with a low-temperature device set to a temperature of 193 K, which was chosen on the basis of the data collection temperature reported for the known crystal form. Warming similarly grown crystals to room temperature did not result in the formation of another phase. Since the sample was cooled by contact with a cotton bud soaked in liquid nitrogen, heating and cooling rates could not be monitored but were generally fast.

Crystallisation using a Linkam stage: α- β- and γ-phases

To improve the temperature control, we switched to a Linkam THMS600 heating and freezing stage, which enables temperature

control within a precision of 0.1 K while still being able to view the sample through a quartz glass window (Fig. 3). Prior to sample cooling, the stage was heated to 373 K to remove any moisture trapped inside the sample chamber. Phase assignment was performed by a combination of single-crystal X-ray diffraction and Raman spectroscopy. Over 50 crystallisation trials were performed. Depending on the starting crystalline phase, several transition paths are possible: herein, we detail five crystallisation protocols. (1) The α-form was reproducibly obtained by cooling the sample below its glass transition temperature and then heating it up to a temperature in the range of 228–248 K, irrespective of the heating rate. Once formed, fast heating rates suppressed any further transition. (2) Starting from the α-phase and using a slow heating rate (0.5 K min^{-1}) a transition to the β-phase occurred at *ca.* 248 K, in good agreement with the value of 250.3 K reported by Endo *et al.*[18] (3) Starting from a fully crystalline sample of the α-phase (*i.e.* in the absence of any liquid), following an isothermal run at 258 K for 10–20 min, a transition to the γ-phase was sometimes observed. (4) The γ-phase was, at times, also obtained directly from the β-form using a similar isothermal run. (5) The γ-phase, which has the lowest crystal growth rate, was reproducibly obtained by leaving the sample at 277 K for a few days. As reported by Endo *et al.*,[19] the activation energy of the β → γ phase change is considerable; hence, a long isothermal phase may be a key factor for either direct nucleation of the γ-phase from the liquid state or for the β → γ transition. Considerations on the reproducibility of the crystallisation protocols are further explored in the Results and discussion section.

Single-crystal X-ray diffraction

Full details on the programs used for data reduction and structure refinement can be found in the ESI.† Structure refinement strategies are discussed in detail in the ESI† and only the most salient features are reported below. Crystallographic data are reported in Table 2.

α-Phase

Sample transfer to the diffractometer proved to be particularly difficult for this phase as any mechanical interference with the crystal at high enough temperatures where the crystal could be manipulated resulted in a phase transition. A suitable crystal for diffraction was hence grown on a secondary glass shard support placed on the Linkam stage and the shard was subsequently mounted on a Bruker SMART 6000 Apex II CCD diffractometer (Fig. 3). Diffraction data were collected using Cu Kα radiation of $\lambda = 1.54178$ Å from a rotating anode at 100(2) and 193(2) K. The structure at 100 K was found to be ordered. At 193 K disorder could be modelled for the $[PF_6]^-$ anion and for C8 and C9 of the butyl side chain using two-site split models.

β-Phase

Diffraction data were collected using a Bruker AXS SMART Apex II CCD diffractometer equipped with Mo-Kα sealed-tube radiation of $\lambda = 0.71073$ Å for an *in situ* grown crystal contained in a capillary at 193(2) K. A similar diffractometer equipped with a Ag microsource (Incoatec) of $\lambda = 0.56085$ Å was used for the 293(2) K high-pressure DAC experiment. Both low-temperature and high-pressure structures were found to be pseudo-merohedral triclinic twins, with unit-cell constants emulating a monoclinic *C* metric cell and a $[\bar{1}\ 1\ 0]$ twin direction. Both $[PF_6]^-$ anions were found to be equally disordered over two positions. Disorder was additionally found in the butyl side chain of the cations: for C10 at low temperature and for C9, C10 and C20 at high pressure.

γ-Phase

Diffraction data were collected on a single crystal grown on the Linkam stage and transferred to a Bruker AXS SMART Apex II CCD diffractometer with Mo-Kα sealed-tube radiation of $\lambda = 0.71073$ Å at 263(2) K. A minor but significant disordered component of the butyl side chain, atoms C8 and C9, could be successfully refined using a split-site model.

Raman spectroscopy

Raman spectra were recorded with a Horiba Jobin Yvon HR800 UV Micro-Raman spectrometer equipped with an air-cooled 20 mW 488 nm Ar-laser. Raman spectra were collected in the 200–1200 cm^{-1} range with a spectral resolution of *ca.* 2.2 cm^{-1} using a grating of 600 grooves per mm and a Peltier-cooled CCD detector (Andor, 1024 × 256 pixels). The spectra were calibrated with the Raman scattering frequency of Si before and after each measurement.

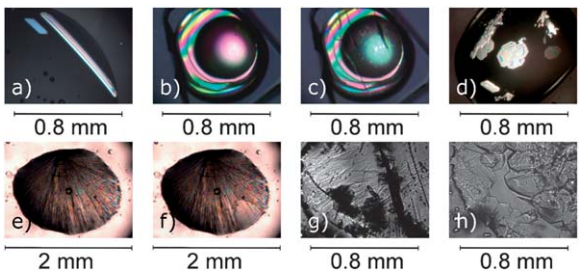

Fig. 3 Optical images of crystals of [bmim][PF_6] grown on a Linkam stage. (a) Single crystals of the α-phase growing from the liquid at 262 K; (b) single crystal of the α-phase at 260 K grown on a glass shard (coexistence of liquid and solid), and (c) crystal after cooling to 203 K; (d) β-phase melting at 279 K; (e) initial and (f) final stages of the α → β phase transition at 248 K; (g) nucleation of the γ-phase from the β-phase at 258 K and (h) γ-phase coexisting with the melt at 282 K.

Results and discussion

Conformation of the $[bmim]^+$ cation in the solid state

In the present discussion, the rotamer denomination follows the scheme outlined by Tsuzuki *et al.*,[20] which is based on the C2–N1–C7–C8 torsion angle (Fig. 1) being positive. The conformations of the N1–C7–C8–C9 and C7–C8–C9–C10 torsion angles, θ_1 and θ_2, respectively, are then assigned to the following angle ranges: T (*trans*, −150 to +150°), G (*gauche*, +30 to +90°) and G′ (*gauche*′, −30 to −90°), see Fig. 4 for details. As noted by Endo *et al.*,[18] the three polymorphs of [bmim][PF_6] can be identified on the basis of characteristic Raman bands: for the

Table 2 Crystallographic data for the three polymorphs of [bmim][PF_6] discussed in this paper

Structure	α	α	β	β	γ	γ
Pressure	0.1 MPa	0.1 MPa	0.1 MPa	0.07 GPa	0.1 MPa	0.1 MPa
T/K	100(2)	193(2)	193(2)	293(2)	180–193[a]	263(2)
Ref.	This work	This work	This work	This work	MAZXOB01[17]	This work
Space group	*Pbca*	*Pbca*	$P\bar{1}$	$P\bar{1}$	$P\bar{1}$	$P\bar{1}$
a/Å	9.3855(3)	9.4924(5)	9.3869(8)	9.5818(13)	8.774(5)	8.8215(8)
b/Å	9.7769(3)	9.8406(5)	9.5879(8)	9.5826(9)	8.944(9)	9.0796(9)
c/Å	26.7170(7)	26.8817(13)	14.4964(12)	14.5801(10)	9.032(6)	9.0381(8)
α/°	90	90	98.492(5)	99.219(10)	95.95(2)	96.671(7)
β/°	90	90	98.354(6)	99.252(6)	114.93(1)	114.768(6)
γ/°	90	90	101.089(6)	99.667(10)	103.01(3)	103.071(7)
V/Å^3	2451.58(13)	2511.0(2)	1245.85(18)	1278.2(2)	610.2(8)	621.82(10)
Z'	1	1	2	2	1	1
D_c/g cm^{-3}	1.540	1.503	1.515	1.477	1.55	1.518
Measured reflections	24 529	28 075	18 072	10 400	6680	7824
Unique reflections	2380	2427	3544	1063	3484	2291
Observed reflections[b]	2254	2054	2711	815	n.a.	1624
Parameters/restraints	156/0	229/255	349/618	341/809	154/0	174/57
R_{int}	0.05	0.06	0.05	0.04	n.a.	0.02
R	0.037	0.048	0.084	0.074	0.045	0.050
wR	0.100	0.155	0.275	0.2113	0.128	0.145
$\Delta\rho_{min/max}$/e$^-$ Å^{-3}	−0.31/0.33	−0.39/0.27	−0.41/0.52	−0.14/0.18	−0.29/0.33	−0.34/0.42

[a] Three different temperatures are given in the paper (193 K), ESI (180 K) and CIF file (183 K). [b] Criteria for observed reflections: $I > 2\sigma(I)$.

α-phase a band at 338 cm^{-1}, associated with ring wagging and chain deformation;[29] for the β-phase a band at 624 cm^{-1}, which is associated with a number of group vibrational modes;[30] for the γ-phase a band at 326 cm^{-1}, presumably also associated with ring wagging and chain deformation. Endo *et al.*[18] note that these bands are characteristic fingerprints for the GT, TT and G′T conformers, respectively. Our experimental Raman spectra, shown in Fig. 5, are in very good agreement with those reported at low temperature by Endo *et al.*[18] and at high pressure by Russina *et al.*[21]

Whilst Raman spectroscopy enables a rapid and unambiguous phase assignment, single-crystal X-ray diffraction allows the determination of a more detailed description of the cation conformation in the solid state. Gas-phase calculations on the cation, in isolation and in the presence of counterions have shown that the nine lowest-energy rotamers adopt a combination of the T, G and G′ torsion angles, and that the energy of all rotamers are within 5 kJ mol^{-1} of each other;[20] however, our crystallographic study points out to the existence of other conformers, which in the previous calculations correspond to saddle points on the torsional potentials, so that additional torsion angles are introduced here: S (*syn*, −30 to +30°), E (*eclipsed*, +90 to +150°) and E′ (*eclipsed′*, −90 to −150°). The

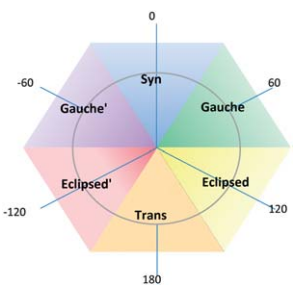

Fig. 4 Dihedral angles for N1–C7–C8–C9 and C7–C8–C9–C10 for defining the [bmim]$^+$ cation conformation.

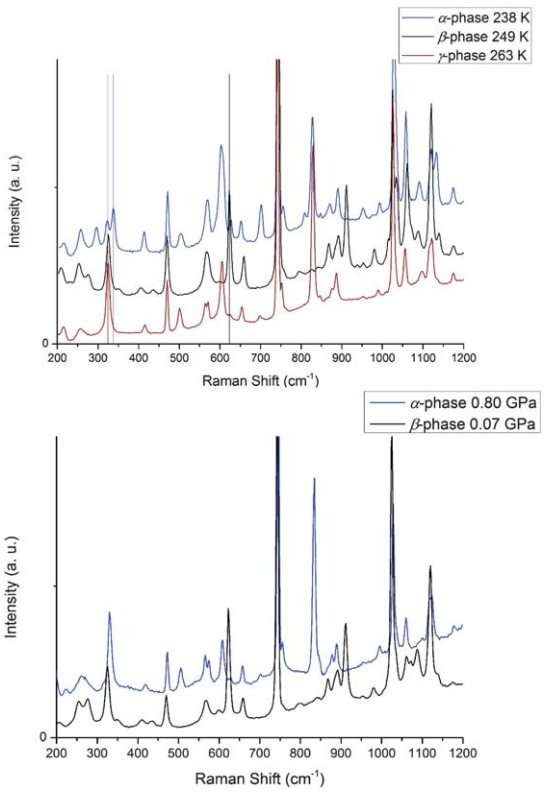

Fig. 5 Raman spectra of [bmim][PF_6] polymorphs collected at different conditions of temperature (top) and pressure (bottom). Solid lines highlight the frequencies of the characteristic bands below 800 cm^{-1} for the α-, β- and γ-forms at 338, 624 and 326 cm^{-1}, respectively.

values for the torsion angles θ_1 and θ_2 observed from single-crystal diffraction are summarised in Table 3.

The conformers of the α- and γ-phases are confirmed to be GT and G′T, respectively. The coexistence of the GT and G′T conformers in the α-phase, suggested by Endo *et al.*[18] on the basis of variable-temperature Raman spectroscopy can also be rationalised: the single-crystal structure at 193 K indicates the presence of a minor (25%) component attributed to the G′T conformer. On further cooling the same crystal, the disorder disappears and the observed conformation is entirely GT. This observation points towards the presence of dynamic disorder in the cation, though ideally more data points should be collected to confirm this. Dynamic disorder or enhanced thermal motion in the cation is, to a lesser extent, also present in the γ-form: whilst the structures reported by Dibrov and Kochi[16] and Choudhury *et al.*[17] determined below 200 K indicate that the cation conformer is G′T, our 263 K structure additionally shows the presence of a minor GT component (8%). Multiple conformations are also observed for the two molecules in the asymmetric unit of the β-phase at 193 K/0.1 MPa and at 293 K/0.07 GPa. When considering the main disordered components only, the conformations of the $[bmim]^+$ cation at 193 K/0.1 MPa and at 293 K/0.07 GPa are best described as TG′/TT and TT/TT, respectively. When the minor disordered components are also taken into account, the description becomes TG′ (30%TE′)/TT at low temperature and TT (30%TE′)/TT (30%TE′) at high pressure. Crystal structures of ionic liquids crystallising with more than one molecule in the asymmetric unit do in fact often contain different conformers; the E and E′ conformers are considerably less common compared to the T, G and G′ counterparts, but not unknown. A search for $[bmim]^+$ containing structures in the current version of the Cambridge Structural Database (the CSD, V. 5.33 including updates to August 2012, was searched for structure containing the $[bmim]^+$ cation with available 3-D coordinates, an *R*-factor below 10%, no errors and excluding powder structures) reveals that out of a total of 96 structures (90 unique), 1 contains twelve $[bmim]^+$ cations in the asymmetric unit, another contains five, 9 contain four, 2 contain three and 19 contain two. The distribution of the observed conformers is shown in Fig. 6. The wide range of different conformations observed in different polymorphs and in the same phase at different conditions of pressure and temperature is a further indication of the low barrier to rotational isomerism. In a very recent solid-state ^{1}H NMR relaxation experiment study Endo *et al.*[19] reported that the averaged mobility of the cation follows the order $\gamma < \beta \leq \alpha$ and that the same trend is also followed by the slow segmented motion of the butyl group. These findings are in general good agreement with our observations; moreover, in most cases the motions seem to be larger than librational motions and are associated with conformational changes of the butyl group.

The TT conformer assignment for the β-phase by Endo *et al.* and Russina *et al.* on the basis of Raman data is essentially correct when considering the major disorder component; however, the availability of single-crystal data provides a higher level of detail. The model presented, herein, still represents an averaged model: the data do not allow a deconvolution of electron density and thermal motion and the given values should be taken as guidelines; in reality it is possible that a range of conformations between TG′ and TE′ exist in the crystal, in particular as a function of varying temperature and pressure.

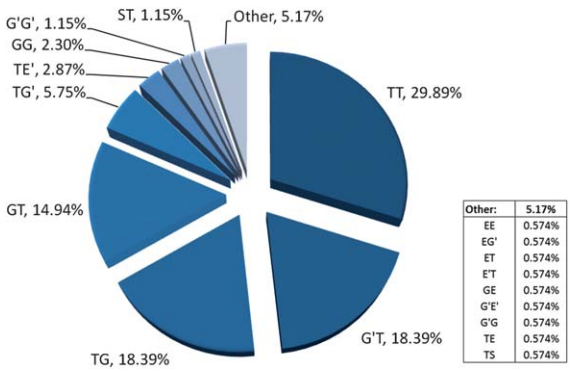

Fig. 6 Distribution of the conformers of $[bmim]^+$-containing structures found in the CSD.

Table 3 Torsion angles and cation conformation for the polymorphs of $[bmim][PF_6]$ at different experimental conditions

	α(100 K)	α(193 K)	β(193 K)	β(0.07 GPa)	γ(193 K)[17]	γ(263 K)
θ_1(N1–C7–C8–C9)/° (molecule 1)	63.65(19)	63.5(5)[a] [−54.1(14)]	179.8(12)	168(2) [−164(3)]	−60.80(17)	−60.3(5) [56(4)]
θ_1(N11–C17–C18–C19)/° (molecule 2[b])			167.5(8)	168(2)		
θ_2(C7–C8–C9–C10)/° (molecule 1)	176.76(14)	176.2(3) [−176.0(8)]	−64.4(19) [−104(2)]	166(3) [−135(3)]	−178.05(17)	−176.4(3) [173(3)]
θ_2(C17–C18–C19–C20)/° (molecule 2)			180.0(8)	−178(3) [−122(4)]		
Conformation molecule 1	GT	GT [25% G′T]	TG′ [30% TE′]	TT [30% TE′]	G′T	G′T [8% GT]
Conformation molecule 2			TT	TT [30% TE′]		

[a] Values in square brackets refer to the minor disordered component. [b] Two molecules in the asymmetric unit for the β-form.

Disorder of the $[PF_6]^-$ anion in the solid state

Rotational disorder of the $[PF_6]^-$ group is often observed in the solid state, as expected for a highly symmetric molecule. At 193 K the only crystalline phase which does not show evidence of anion disorder is that of γ, which incidentally is also the most dense phase at this temperature. In the α-phase the nature of the anion disorder is most likely to be dynamic, as exemplified by the ordering observed on cooling the single-crystal from 193 to 100 K. In the β-phase the two crystallographically independent anions are both extensively disordered about axial F–P–F bonds. The trends in the anion disorder in the crystalline state are in agreement with the results of the spin-lattice rotational dynamics study of Endo *et al.*[19] A more detailed description of anion disorder can be found the ESI.†

The crystal structures of the three polymorphs

The structure of the γ-phase determined at 263 K is in very good agreement with the low-temperature structure reported previously. The crystal packing in this form is based on two primary building blocks of centrosymmetric cation dimers. In the first, here termed "closed" dimer, the butyl groups are pointing inwards, *i.e.* towards the space between two imidazolium rings, and in the second, "open" dimer, they are pointing outwards (Fig. 7). Both types of packing arrangements are found in short- and long-chain ionic liquids.[11,31,32] In long alkyl structures, "closed" dimers favour hydrophobic alkyl–alkyl interactions. The β-phase also exhibits both types of packing arrangements: the "open" dimer is formed between symmetry equivalent molecules, whilst the "closed" one, a pseudo-centrosymmetric dimer, is formed between symmetry-independent molecules. In contrast to the γ- and β-forms, the α-phase only exhibits one type of centrosymmetric dimeric arrangement, namely the "open" dimer; in addition, a different, less compact closed dimer, with molecules related by glide symmetry, is formed. The nature of the "open" dimer also changes across the three structures: in the α- and β-phases the methyl groups of the imidazolium ring are aligned, whereas in the γ-form the butyl groups are. When considering the entire crystal packing, an overall change from a mixed short-alkyl/long-alkyl to a long-alkyl structure-type packing arrangement is observed when going from the γ- through the β- to the α-phase. The phase that crystallises at the lowest temperature from the supercooled liquid state adopts a packing arrangement that is more akin to that encountered in long-alkyl chain hexafluorophosphate ionic liquids (Fig. 8), with layers of interacting butyl side chains separated by *c*/2, similar to what was previously predicted for this compound.[9] This is in line with the thermodynamic data of Triolo *et al.*,[9] who determined that the supercooled liquid-fragility index of [bmim][PF_6] is similar to that of longer side chain 1-alkyl-3-methyl imidazolium-based salts.[33]

The geometric parameters describing the centrosymmetric dimeric arrangements are detailed in Table S1 (see ESI for details†). π–π stacking of cation dimers is observed between dimers in the "open" arrangement, and the smallest offset to perfect stacking is found in the β-phase [2.342 Å at 193 K compared to 3.543 and 3.394 Å in the α- and γ-phases, respectively, at the same temperature], although the interplanar

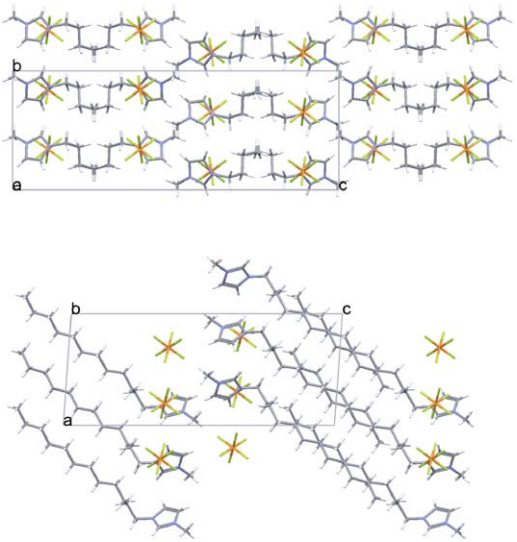

Fig. 8 Crystal packing of [bmim][PF_6], α-form (top) and of 1-*n*-dodecyl-3-methylimidazolium hexafluorophosphate,[32] CSD Ref. code HIWNOQ (bottom).

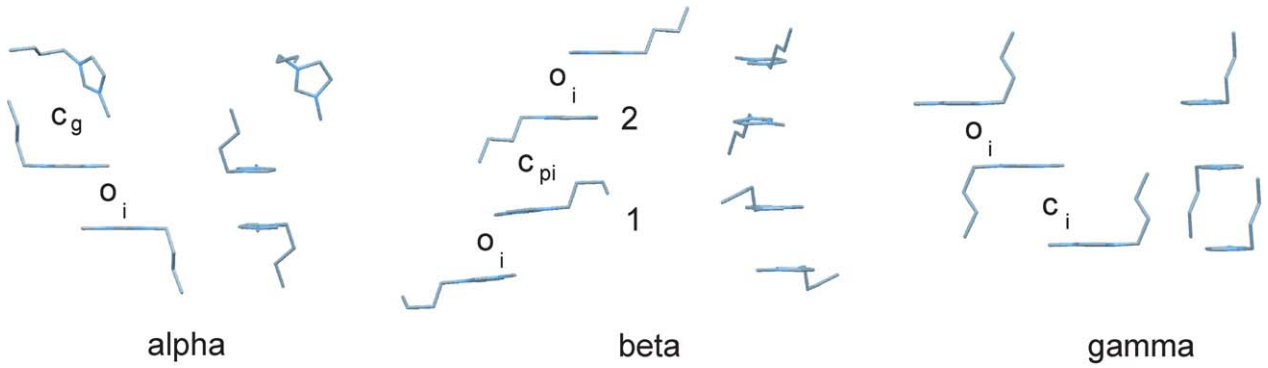

Fig. 7 Dimeric arrangements in the three polymorphs of [bmim][PF_6] viewed along two different stacking directions. Anions, H-atoms and minor disorder components have been omitted for clarity. o_i = centrosymmetric "open" dimer, c_i = centrosymmetric "closed" dimer, c_{pi} = pseudo-centrosymmetric "closed" dimer, c_g = glide "closed" dimer. Symmetry-independent molecules in the β-phase are labelled 1 and 2.

distance is also the longest. At 193 K, the interplanar distance for the "closed" dimer is shortest in the γ-phase [4.3688(9) Å compared to 5.452(4) Å in the β-phase]. From Table S1† the more pronounced pseudo-symmetry in the β-form at high pressure is evident: all parameters describing the "open" dimers between symmetry inequivalent molecules are more similar at high pressure than they are at low temperature.

The $[PF_6]^-$ anions contribute to structural stability by linking the dimeric arrangements *via* several F···H contacts. In the structures of the γ- and β-phases, the anions occupy the space between the stacked cation columns, whilst in the structure of the α-phase the structure motifs formed by cations and anions are intertwined. Void analysis (performed with the program Mercury[34]) reveals that whilst this space forms continuous columns along the *b*-axis in the γ-form, it gradually moves into a double-pocket arrangement and finally into segregated individual pockets that fit a single anion on going from γ to β and from β to α (Fig. 9).

Interestingly, at 0.07 GPa the density of the β-phase is *ca.* 2.5% less than the corresponding density of the same phase at 193 K. Isothermal compression at 293 K to *ca.* 0.35 GPa, leads to a density increase of *ca.* 3.4% from 1.477 to 1.527 g cm^{-3} (full structural data not reported here). The effect of decreasing temperature on the crystals of the γ- and α-phases is to form denser structures. The considerable variation of density as a function of temperature is indicative of the "softness" of the intermolecular interactions that govern crystal packing.

The attractive energy between imidazolium-based cations and anions is predominantly attributable to Coulombic forces. The contact involving the acidic C2–H2 bond and the anion is generally accepted as a hydrogen bond, albeit weak in the case of $[PF_6]^-$.[35,36] Tsuzuki *et al.*, have shown by computational methods that hydrogen bonds in ionic liquids involving imidazolium ring hydrogens are not directional and are mainly governed by the distance between the ring hydrogen and the anion. In a subsequent publication, the authors have shown that a contact between a Br^- anion and the C2–H2 group stabilises the GT $[bmim]^+$ cation conformer, whilst close contacts to C4–H4 and C5–H5 do not alter the relative stability of the GT, G′T and TT conformers.[20] H···F contacts less than the sum of the van der Waals radii are given in Table S2 (see ESI for details†). From this table it can be seen that the coordination number of the cation and anion varies across temperature, pressure and crystal phase. Within the same phase, the coordination numbers are inversely proportional to crystal density; the higher density observed at low temperature is achieved by an increase in the number of close H···F contacts, defined as contacts whose distance is smaller than the sum of the van der Waals radii. The crystal density at 193 K follows the order $\alpha < \beta \ll \gamma$; the same order is observed in the number of close H···F contacts, whilst the order is $\alpha \sim \gamma > \beta$ when considering both the coordination number of cations and anions. These results are in fairly good agreement with the strength of cation–anion interactions estimated from Raman spectroscopy that follows the trend $\gamma > \beta \geq \alpha$.[19]

All three crystalline phases are characterised by C···F contacts involving H2 to two anions on either side of the imidazolium ring. The anion is defined to lie above the ring when it is on the same side of the butyl chain and below when on the opposite side. Details of the geometric parameters for these contacts are given in the ESI (Table S3†). At 193 K, short C2···F distances are observed for the α-form [two contacts to disordered F-atoms at 3.062(6) and 3.064(9) Å to the anion below the ring; note that at 2.993(10) and 3.029(8) Å, C···F contacts to the anion above the ring are shorter but H···F distances are greater than the sum of the van der Waals radii]. In the γ-form the corresponding distance is slightly longer [3.192(4) Å]; in this form, the distance to the anion above the ring is comparatively longer [3.233(5) Å] but more linear (C2–H2···F angle 152 and 120°, respectively). In the β-form a wider range of distances to anions involving H2 are observed because of the presence of two molecules in the asymmetric unit and extensive anion disorder, thereby making contact analysis more complex. For instance, at 193 K the shortest distance has a value of 2.921(16) Å and involves molecule 2 and the anion below the imidazolium ring; the disordered counterpart is longer [3.031(17)] Å and at 2.84 Å the H···F distance is greater than the sum of the van der Waals radii; the associated contact angles are 99 and 92°, respectively. At 0.07 GPa and ambient temperature, the corresponding distances and angles are 2.74(3) Å, 112° and 3.19(3) Å, 118°,

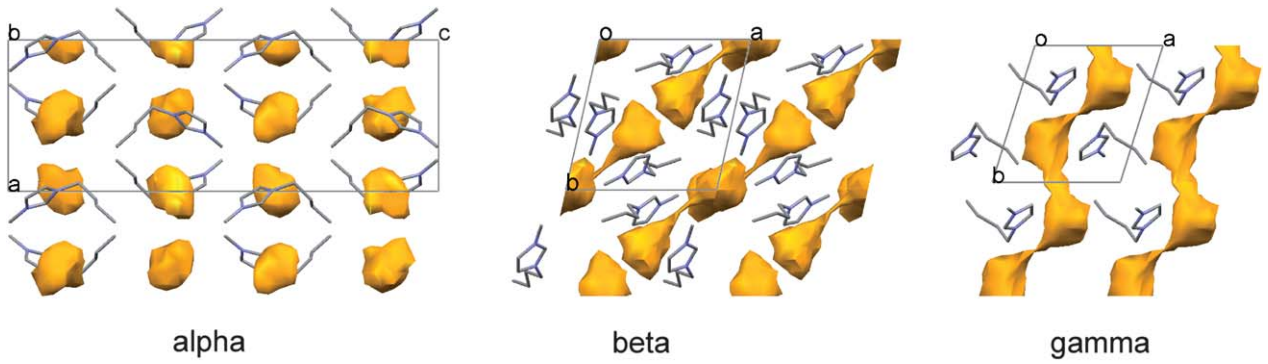

Fig. 9 Crystal packing in the three polymorphs of $[bmim][PF_6]$. H-atoms and disordered atoms have been omitted for clarity. The space occupied by the anions is depicted by solvent accessible void surfaces generated with the program Mercury (probe radius = 1.2 Å, grid spacing = 0.7 Å). Solvent accessible void volume at 193 K expressed as % unit cell volume: 5.1% in the α-, 5.3% in the β- and 4.4% in the γ-polymorph, respectively.

respectively, and all H···F distances are less than the sum of the van der Waals radii. At high pressure, the number of short H···F contacts is lower than at low temperature, in line with the lower density, and the environment around the symmetry independent molecules more similar when considering average values, in line with the higher pseudo-symmetry.

All three polymorphs exhibit close contacts that involve not only H2 but all ring as well as the methyl hydrogen atoms; overall, the more linear contacts are associated with longer C···F distances. The former observation seems to suggest that close contacts between these atoms and anions are not directly responsible for the observed cation conformation in the solid state. On inspection of Tables S2 and S3 deposited as ESI† other more indicative trends emerge. The GT conformer appears to be stabilised by a contact to the hydrogen atom attached to C7 and no contacts to C8 or C10 (for which distances are >3.7 Å); the G′T conformer is additionally stabilised to contacts to C10 (the contact to H8 observed at 193 K is long: H8···F distance = 2.67 Å and C8···F distance = 3.662(5) Å). The difference between the TT, TG′ and TE′ conformers is not immediately evident but all involve additional contacts to the terminal butyl carbon atom. Differences in the number of contacts involving methyl hydrogen atoms are inconclusive given that their positions are not reliable.

General discussion

Our experiments indicate that the α-polymorph is very sensitive to temperature changes and should be kept well below the transition temperatures to the β- or γ-phases. The temperature range used for *in situ* crystallisation followed by crystal growth on a diffractometer by zone melting, *e.g.* using an OHCD apparatus, is usually quite large and difficult to control: this could partially explain why single-crystal structures reported in the literature correspond to the γ-phase despite the fact that the crystal was grown at temperatures where the α-phase is stable.[17] The reproducibility of the crystallisation protocols outlined in the Experimental section seems to be strongly dependent on a number of factors, including sample volume, water contamination and coexistence of liquid and solid phases. For instance, nucleation of the α-phase is most reproducible with sample volumes greater than *ca.* 200 μL; similarly, crystallisation of the β-phase appears to be more reproducible when the sample is contained in a capillary and the heating rates are high. Protocols 3 and 4 outlined in the Experimental section are most successful when the whole sample is crystalline: when the liquid and crystalline phases coexist, the α to liquid phase transition can occur at *ca.* 263 K, without a prior solid–solid phase transition. The presence of water as a contaminant, either as a liquid or as ice, also seems to facilitate the formation of the γ-form, though this has not been tested systematically. Interestingly, the presence of water also seems to be crucial for the crystallisation of the γ-phase under high-pressure conditions: preliminary experiments indicate that crystallisation of [bmim][PF_6] from very diluted aqueous solutions in the 0.4–0.7 GPa pressure range results in the formation of the γ-form, as confirmed by single-crystal X-ray diffraction. In line with other authors, on increasing pressure, we did not observe the crystallisation of the γ-phase from the pure liquid, suggesting that, based on density differences, the application of modest pressure favours crystallisation of the β-phase.

The existence of multiple conformers in the liquid state of [bmim][PF_6] is well documented.[18,37] A recent elegant study by Jeon *el al.* reported the nanocrystallisation of [bmim][PF_6] at the vapour–liquid interface at 310 K by grazing-angle synchrotron X-ray diffraction.[38] The sharp Bragg diffraction peaks observed by the authors, arising from nanocrystallites at the interface and coexisting with the broad diffraction features of the liquid, were indexed and a quasi-2D long-range ordered structure was extracted which was similar to that of the γ-form. Whilst we also observe coexistence of crystalline and liquid states at certain conditions of temperature and pressure, our discrete Bragg reflections collected in transmission geometry are very starkly dominated by the crystalline bulk: hence, the cation and anion disorder were analysed in terms of crystalline disorder. Surface diffraction methods could shed more light into the nature of the crystal–liquid interfaces. It could be conceivable, in particular for the β-phase, where disorder is more severe, that different cooling rates would result in a different distribution of conformers – however, data collected on different crystals suggest that the differences are not significant, so that the main trends reported are confirmed.

As indicated in the Experimental section, crystals of the β-phase obtained at high-pressure or low-temperature conditions are characterised by twinning. The β-phase was found to be stable between *ca.* 0.07 and 0.4 GPa. As expected, the lowest deviation from perfect monoclinic *C* symmetry was observed for the high-pressure structure collected at 0.07 GPa, *i.e.* at phase-boundary conditions, and this is also the structure exhibiting the highest degree of pseudo-symmetry and perfect domain overlap. Further compression of the single crystal from 0.07 to 0.35 GPa resulted in a unit-cell with a higher degree of deviation from a perfect monoclinic *C* cell, see ESI† for details. This is a small pressure range to probe the effects of pressure on disorder; however, our data analysis indicates no significant changes in disorder on increasing pressure.

Whilst the study of conformational flexibility and energetic aspects of the $[bmim]^+$ cation in the gas phase are useful, it is clear that an extrapolation of the findings to structures adopted in the solid state is not entirely justified since DFT gas phase calculations on isolated cations ignore the effects of anions and the stabilising energy contributions that arise from crystal packing. It should be noted that whilst Tsuzuki *et al.* have studied anion effects in their conformational analysis, the $[PF_6]^-$ anion was not included in the calculations. Hence, whilst the three most stable conformers in the gas phase are GT (0.02 kcal mol^{-1}), TT (0.00 kcal mol^{-1}) and G′T (−0.50 kcal mol^{-1}) (geometries optimised at the MP2/6-311G** level and relative energies estimated at the CCSD(T)/cc-pVTZ level), the TG′ conformer observed for one of the two independent molecules in the β-phase at 193 K is only *ca.* 4 kJ mol^{-1} less stable than the G′T rotamer and such a small barrier to rotation can be easily overcome by other stabilising intermolecular interactions in the solid state. The phenomenon of conformational polymorphism in the solid state has been well documented in the literature.

Nangia summarises this very nicely: "organic molecules with flexible torsions and low-energy conformers have a greater likelihood of exhibiting polymorphism because (1) different conformations lead to new hydrogen bonding and close-packing modes and (2) the tradeoff reduces the total energy difference between alternative crystal structures".[39] These observations are also applicable in the case of the title compound and confirmed by the values of the phase transition enthalpies from DSC measurements.[18] Whilst it would be interesting to compare the difference in lattice and interaction energies of the three polymorphs by means of computational calculations, the observed disorder would make the analysis more difficult, and such a study is beyond the scope of this paper. Despite the widespread conformational flexibility of the alkyl side chain and the large number of structures available in the CSD, there are not many examples of polymorphs reported for ionic liquids, but those reported are conformational polymorphs; the low incidence of polymorphic structures might be partially due to the fact that the polymorphism of these compounds has not been extensively investigated; for examples see refs. 11, 31, 32 and 40–42.

Although the γ- and α-phases exhibit very similar Raman spectra, their crystal structures are profoundly different. The crystal structures of the three polymorphs are substantially different from one another: hence, X-ray powder diffraction can be an effective tool for rapid phase identification. Two forms were previously identified by Triolo *et al.*[9] using wide-angle X-ray scattering (cr-I and cr-II, see Table 1). Comparison of simulated patterns (see Fig. S4 in the ESI†) derived from the single-crystal structures of the three forms with the patterns reported in this previous paper indicates the following: the patterns labelled cr-I (see Fig. 8, 9 and 10 of the original paper) correspond to the α-phase, whilst the patterns labelled cr-II correspond to the γ-phase (see Fig. 9 and 10 of the original paper). The β-form was not reported. It is interesting to note that the powder data clearly indicate the occurrence of the α → γ transition at 250 K, also confirmed by thermal analysis, despite the fact that a similar temperature was reported for the α → β transition by Endo *et al.* Our experiments confirm that sample thermal history, impurities and heating/cooling rates are important factors affecting the polymorphic phase transitions in [bmim][PF_6].

Conclusions

The polymorphic behaviour of the ionic liquid [bmim][PF_6] has been studied by Raman spectroscopy, single-crystal X-ray diffraction and optical microscopy. The existence of three polymorphs, α, β and γ, which can be crystallised as a function of low temperature or high pressure, has been confirmed and all three have been structurally characterised. The conformational flexibility of the $[bmim]^+$ cation, together with the capability of rotational disorder of the $[PF_6]^-$ anion, give rise to different conformations in the solid state not only as a function of crystallisation conditions but also of changes in temperature and pressure to the same phase. The range of cation conformations identified provides a basis by which to validate simulation and modelling data for both fundamental studies and process design. The GT, TT and G′T conformations of the cation in the α-, β- and γ-phases, respectively, inferred from previous analysis of Raman stretching frequency, is essentially confirmed; however, the availability for the first time of single-crystal X-ray data for all polymorphs reveals a wider range of conformers than previously thought. Across the three phases and under different experimental conditions, a large variation in crystal packing densities and in structural disorder is observed. These variations are likely contributing driving forces for the polymorphic interconversions. Whilst phase transitions do not occur in a single-crystal-to-single-crystal fashion and the molecular packing arrangements of the three forms are very distinct, some continuity in the structural motifs of the building blocks is observed.

Acknowledgements

This work was carried out with the financial support of the Deutsche Forschungsgemeinschaft (DFG Emmy Noether Grant FA 964/1-1), the EPSRC (EP/G012156/1) and Merck GMbH. We would like to thank: Prof. Dietmar Stalke and his group (Göttingen) for access to the Ag microsource, Prof. George M. Sheldrick and Dr Birger Dittrich (Göttingen) for access to the Cu rotating anode, Dr Junfeng Qin (Göttingen) for initial assistance with Raman measurements, Drs Heidrun Sowa and Regine Herbst-Irmer (Göttingen) as well as Michael Ruf (Madison) for useful discussions, Ulf Kahmann and Heiner Bartels for technical assistance and Prof. Simon Parsons (Edinburgh) for a copy of SHADE.

Notes and references

1 M. J. Earle and K. R. Seddon, *Pure Appl. Chem.*, 2000, **72**(7), 1391.
2 P. Wasserscheid and T. Welton, *Ionic Liquids in Synthesis*, Wiley-VCH, Weinheim, 2007.
3 V. I. Parvulescu and C. Hardacre, *Chem. Rev.*, 2007, **107**(6), 2615.
4 W. M. Reichert, J. D. Holbrey, K. B. Vigour, T. D. Morgan, G. A. Broker and R. D. Rogers, *Chem. Commun.*, 2006, 4767.
5 R. A. Judge, S. Takahashi, K. L. Longenecker, E. H. Fry, C. Abad-Zapatero and M. L. Chiu, *Cryst. Growth Des.*, 2009, **9**(8), 3463.
6 J.-H. An, J.-M. Kim, S.-M. Chang and W.-S. Kim, *Cryst. Growth Des.*, 2010, **10**, 3044.
7 T. G. A. Youngs, C. Hardacre and C. L. Mullan, *Ionic Liquids in Chemical Analysis*, CRC Press, Boca Raton, FL, 2008, p. 73.
8 C. Hardacre, J. D. Holbrey, M. Nieuwenhuyzen and T. G. A. Youngs, *Acc. Chem. Res.*, 2007, **40**, 1146.
9 A. Triolo, O. Russina, C. Hardacre, M. Nieuwenhuyzen, M. A. Gonzalez and H. Grimm, *J. Phys. Chem. B*, 2005, **109**, 22061.
10 F. H. Allen, *Acta Crystallogr., Sect. B: Struct. Sci.*, 2002, **58**, 380.
11 J. D. Holbrey, W. M. Reichert, M. Nieuwenhuyzen, S. Johnston, K. R. Seddon and R. D. Rogers, *Chem. Commun.*, 2003, 1636.

12 B. L. Bhargava and S. Balasubramanian, *J. Chem. Phys.*, 2007, **127**, 114510.
13 B. L. Bhargava and S. Balasubramanian, *J. Phys. Chem. B*, 2007, **111**, 4477.
14 M. Bühl, A. Chaumont, R. Schurhammer and G. Wipff, *J. Phys. Chem. B*, 2005, **109**, 18591.
15 M. G. Del Pópolo, R. M. Lynden-Bell and J. Kohanoff, *J. Phys. Chem. B*, 2005, **109**, 5895.
16 S. M. Dibrov and J. K. Kochi, *Acta Crystallogr., Sect. C: Cryst. Struct. Commun.*, 2005, **62**, o19.
17 A. R. Choudhury, N. Winterton, A. Steiner, A. I. Cooper and K. A. Johnson, *J. Am. Chem. Soc.*, 2005, **127**, 16792.
18 T. Endo, T. Kato, K.-i. Tozaki and K. Nishikawa, *J. Phys. Chem. B*, 2010, **114**, 407.
19 T. Endo, H. Murata, M. Imanari, N. Mizushima, H. Seki and K. Nishikawa, *J. Phys. Chem. B*, 2012, **116**, 3780.
20 S. Tsuzuki, A. A. Arai and K. Nishikawa, *J. Phys. Chem. B*, 2008, **112**, 7739.
21 O. Russina, B. Fazio, C. Schmidt and A. Triolo, *Phys. Chem. Chem. Phys.*, 2011, **13**, 12067.
22 Y. Yoshimura, T. Takekiyo, Y. Imai and H. Abe, in *Ionic Liquids – Classes and Properties*, ed. S. T. Handy, InTech, 2011, ch. 8.
23 L. Su, M. Li, X. Zhu, Z. Wang, Z. Chen, F. Li, Q. Zhou and S. Hong, *J. Phys. Chem. B*, 2010, **114**, 5061.
24 L. Su, L. Li, Y. Hu, C. Yuan, C. Shao and S. Hong, *J. Chem. Phys.*, 2009, **130**, 184503.
25 R. G. de Azevedo, J. Esperanca, V. Najdanovic-Visak, Z. P. Visak, H. J. R. Guedes, M. N. da Ponte and L. P. N. Rebelo, *J. Chem. Eng. Data*, 2005, **50**, 997.
26 Y. Zhao, X. Liu, X. Lu, S. Zhang, J. Wang, H. Wang, G. Gurau, R. D. Rogers, L. Su and H. Li, *J. Phys. Chem. B*, 2012, **116**, 10876.
27 F. P. A. Fabbiani, D. C. Levendis, G. Buth, W. F. Kuhs, N. Shankland and H. Sowa, *CrystEngComm*, 2010, **12**, 2354.
28 G. J. Piermarini, S. Block, J. D. Barnett and R. A. Forman, *J. Appl. Phys.*, 1975, **46**, 2774.
29 R. W. Berg, *Ionic Liquids in Chemical Analysis*, CRC Press, Boca Raton, FL, 2008, p. 307.
30 R. W. Berg, M. Deetlefs, K. R. Seddon, I. Shim and J. M. Thompson, *J. Phys. Chem. B*, 2005, **109**, 19018.
31 A. Downard, M. J. Earle, C. Hardacre, S. E. J. McMath, M. Nieuwenhuyzen and S. Teat, *J. Mater. Chem.*, 1998, **8**, 2627.
32 C. M. Gordon, J. D. Holbrey, A. R. Kennedy and K. R. Seddon, *J. Mater. Chem.*, 1998, **8**, 2627.
33 J. J. Moura Ramos, C. A. M. Afonso and L. C. J. Branco, *J. Therm. Anal. Calorim.*, 2003, **71**, 659.
34 C. F. Macrae, I. J. Bruno, J. A. Chisholm, P. R. Edgington, P. McCabe, E. Pidcock, L. Rodriguez-Monge, R. Taylor, J. van de Streek and P. A. Wood, *J. Appl. Crystallogr.*, 2008, **41**, 466.
35 C. Hardacre, S. E. J. McMath, D. T. Bowron and A. K. Soper, *J. Chem. Phys.*, 2003, **118**, 273.
36 S. Tsuzuki, H. Tokuda and M. Mikami, *Phys. Chem. Chem. Phys.*, 2007, **9**, 4780.
37 M. Macchiagodena, L. Gontrani, F. Ramondo, A. Triolo and R. Caminiti, *J. Chem. Phys.*, 2011, **134**, 114521.
38 Y. Jeon, D. Vaknin, W. Bu, J. Sung, Y. Ouchi, W. Sung and D. Kim, *Phys. Rev. Lett.*, 2012, **108**, 055502.
39 A. Nangia, *Acc. Chem. Res.*, 2008, **41**(5), 595.
40 J. Backer, S. Mihm, B. Mallick, M. Yang, G. Meyer and A.-V. Mudring, *Eur. J. Inorg. Chem.*, 2011, 4089.
41 M. Kawahata, T. Endo, H. Seki, K. Nishikawa and K. Yamaguchi, *Chem. Lett.*, 2009, **38**, 1136.
42 Y. U. Paulechka, G. J. Kabo, A. V. Blokhin, A. S. Shaplov, E. I. Lozinskaya, D. G. Golovanov, K. A. Lyssenko, A. A. Korlyukov and Y. S. Vygodskii, *J. Phys. Chem. B*, 2009, **113**, 9538.

